Antiresonant hollow-core fiber fusion spliced to laser gain fiber for high-power beam delivery

CHARU GOEL[1,#] HUIZI LI[1,#] MUHAMMAD ABU BIN ROSDI[2] WONKEUN CHANG[2] AND SEONGWOO YOO[2]*

[1]The Photonics Institute, Nanyang Technological University, 50 Nanyang Avenue, Singapore, 639798, 2School of Electrical and Electronics Engineering, Nanyang Technological University, 50 Nanyang Avenue, 639798, Singapore
[#]The authors contributed equally to this work
*[*seon.yoo@ntu.edu.sg](mailto:seon.yoo@ntu.edu.sg)*

Received XX Month XXXX; revised XX Month, XXXX; accepted XX Month XXXX; posted XX Month XXXX (Doc. ID XXXXX); published XX Month XXXX

We present the selective excitation of fundamental mode in an antiresonant hollow-core fiber (ARHCF) fusion-spliced with a commercial large mode area (LMA) fiber. By designing and fabricating a single ring ARHCF that is mode-matched to LMA fiber and splicing the two using a CO_2 laser-based splicer, we achieve coupling efficiency of 91.2% into the fundamental mode. We also demonstrate all-fiber integration of ARHCF with a commercial ytterbium-doped fiber in a laser cavity for beam delivery application. Coupling of single mode laser output beam into the fundamental mode of ARHCF is demonstrated with 90.4% efficiency (<0.45 dB loss) for up to 50 W continuous wave beam in a stable and alignment free all-fiber laser setup.

1. INTRODUCTION

Hollow core fibers (HCFs) have attracted significant research in the past two decades because of their unique characteristics [1]. Confinement of mode field primarily to the hollow-core region in these fibers leads to low nonlinearity, ultra-low group velocity dispersion, low sensitivity to temperature and high material damage threshold. These characteristics make HCFs attractive for delivery of high-power laser beams [2], sensing [3], low loss transmission over ultrawide bandwidths [4], nonlinear applications like pulse compression [5] and supercontinuum generation using gas-filled HCFs [6]. Antiresonant hollow core fibers (ARHCFs) belong to a special class of HCFs, wherein light guidance can be explained by the principle of antiresonant reflection in waveguides [7] and inhibited coupling of fundamental core mode with lossy modes of dielectric cladding [8]. The negative curvature of the core boundary enhances the confinement of light to the core region, reducing the spatial overlap of core modes with lossy cladding modes and thereby resulting in low confinement loss [9]. ARHCFs have simpler cladding structure as compared to the photonic bandgap hollow-core fibers and can support larger cores with effective single mode operation due to orders of magnitude higher differential propagation loss for higher order modes (HOMs) [10].

Significant research efforts have been devoted by various research groups to tap the potential of ARHCFs for laser beam delivery. There are reports on up to 300 W continuous wave (CW) power coupled into ARHCF with coupling efficiency of 78-81% [2], and delivery of 7 μJ pulse with 318 kW peak power with 85% coupling efficiency [11] in free-space setups. Fusion splicing between a standard single mode fiber (SMF) and tapered Kagome-type antiresonant fiber has been demonstrated in the past with 76.7% coupling efficiency into the fundamental mode, and the rest coupled into the HOMs [12]. The HOMs in ARHCF suffer high confinement losses and dissipate power thermally, leading to increased temperature at the splice point at high powers and a possible damage [13]. Thus, it is crucial to systematically investigate low loss fundamental mode splicing between an ARHCF and solid core fiber to fully exploit the anticipated benefits of using the ARHCF for beam delivery. A recent report on fusion splicing ARHCFs with SMFs reported splice loss of 1–2 dB from SMF to ARHCF, but it did not detail the fraction of power launched into the fundamental mode of ARHCF [14]. In both [12] and [14], the splice loss in the reverse direction (from ARHCF to SMF) was found to be very high 3.5 dB [12] and 10 dB [14] indicating large mode field mismatch between the two fibers. Authors in [15] and [16] have tapered single mode solid core fibers to match their mode field diameter (MFD) with ARHCF and inserted the tapered SMF into ARHCF core. This method could achieve >90% coupling into 10 cm long ARHCF but the coupled power was spread over various HOMs [15]. When a high-power laser was coupled into a longer (2 m) ARHCF, where the HOMs suffer distributed filtering to cladding region, the transmission efficiency obtained reduced to only 40–47% [16]. Moreover, the temperature in the coating of ARHCF rose to 110 ° C at launch power of 90 W, indicating significant light leakage through ARHCF cladding [16]. Hence, despite the prior studies, there is a significant knowledge gap in achieving a low loss all-fiber connection with ARHCF. This letter reports a low loss splicing method obtained by a customized recipe that enables a robust fundamental mode coupling between an in-house ARHCF and a commercial large mode area fiber. This is achieved with an emphasis on low loss splicing and preserving many desired ARHCF characteristics for a fundamental mode beam delivery.

We have fabricated an ARHCF that is mode-matched to a widely used commercial large mode area solid core fiber (LMA-SCF) with a 25 µm core size. The two fibers were fusion-spliced using a CO_2 laser-based splicer. To achieve lowest splice loss, we have carried out a detailed study of contributing factors -mode field matching, cleave angle of fiber end-face and transverse misalignment, which are critical in deciding splicing efficiency of LMA fibers [17]. We achieved 91.2% coupling efficiency into the fundamental mode of ARHCF fusion spliced with LMA-SCF. This is the first report of coupling light into the fundamental mode of ARHCF with such high efficiency using fusion splicing. The obtained splices were found to be reciprocal and coupling efficiency of >90% (fundamental mode splice loss <0.45 dB) is achieved in both directions. If we take the power launched into HOMs of ARHCF into account, the splice loss can be considered even lower.

The fabricated ARHCF was also spliced with a mode-matched ytterbium-doped fiber (YDF) with Fresnel reflection at the splice point forming the laser cavity. The diffraction-limited laser output beam was selectively coupled into the fundamental mode in the ARHCF with 90.4% efficiency at 50 W CW power. This is the first demonstration of integrating ARHCF with a fiber laser cavity using fusion-splicing. Unique features of HCFs have been tapped in previous demonstrations [18, 19] to achieve passive mode-locking of ultrafast lasers by integrating the HCF within the laser cavity, but in free-space setups. High-efficiency fusion-splicing of ARHCF with active fiber reported in this paper paves way for environmentally stable monolithic setups for achieving the same.

2. THEORETICAL STUDY

The LMA-SCF fiber (LMA-GDF 25/250) considered in this work has a core diameter of 25 µm, outer diameter (O.D.) 250 µm, numerical aperture of 0.065 and fundamental MFD of 19.8 µm at 1.064 µm wavelength. We have designed and fabricated a single-ring, seven tube lattice ARHCF with core diameter 31 µm, O.D. 160 µm, cladding capillary wall thickness 0.78 µm and MFD 23.6 µm. The fiber was drawn using standard stack and draw method. Fig. 1 shows the SEM image of fabricated fiber cross-section and the loss spectrum of its fundamental mode. The fiber exhibits a transmission loss of 0.07 dB/m at 1.064 µm. The fraction of power coupled from one fiber to another (coupling efficiency, η), in the absence of any misalignments at splice point, is governed purely by the modal overlap given by [17]:

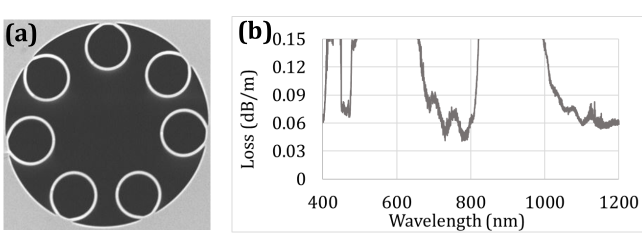

Fig. 1 *a*) SEM image of the cross-section and *b*) loss spectrum of fabricated ARHCF.

$$\eta = \frac{\int E_1^* E_2 dS}{\int E_1^* E_1 dS \int E_2^* E_2 dS} \quad \textbf{(1)}$$

where E_1 and E_2 are the electric field amplitudes of LMA-SCF and ARHCF respectively, and the surface integral is evaluated over the fiber cross-section. If the power in LMA-SCF is confined majorly to its fundamental mode, then the fraction of power coupled into the fundamental mode of ARHCF can be expressed in terms of the fundamental mode field diameters of the two fibers and any misalignments (transverse, longitudinal, angular) that may occur during the splicing [17].

Fig. 2 (a) shows the maximum coupling efficiency achievable from LMA-SCF to ARHCF versus variation in MFD of ARHCF, assuming flat cleaved end-faces in the two fibers and no misalignment at splice point. We note that for the fabricated ARHCF (MFD-23.6 µm), the maximum achievable coupling efficiency between the fundamental modes is ~97%. Commercial splicers can ensure negligible transverse and angular misalignment between the fiber end-faces while splicing. However, angular misalignment due to finite cleave angle of the fiber end-face can be a decisive factor in coupling between LMA fibers [20]. Fig. 2(b) shows the calculated coupling efficiency between the two fibers as a function of the compound cleave angle [17]. We note that even a 0.5 ° compound cleave angle can result in a significant reduction in the theoretical maximum coupling efficiency to 90% for the LMA fibers considered. One also expects additional loss of ~3.3% power because of Fresnel reflection at the interface. In our experiments, we measure coupling efficiency as the ratio of power entering ARHCF and that exiting SCF, so the loss due to Fresnel reflection is accounted for in the input power itself.

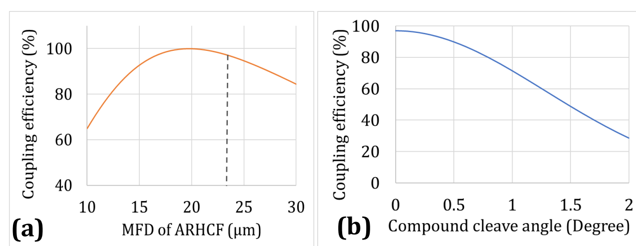

Fig. 2 Maximum achievable coupling efficiency between the fundamental modes of LMA-SCF and ARHCF versus a) MFD of ARHCF and b) compound cleave angle between the two fibers assuming MFD of ARHCF to be 23.6 µm.

3. EXPERIMENTAL RESULTS

A. Splicing with passive LMA

The LMA-SCF and fabricated ARHCF were spliced using commercial CO_2 laser-based glass processing station *Fujikura LZM 100*. Since the two fibers differ in their outer diameters and the ARHCF has large air-fraction with delicate capillary structure to preserve, the SCF is positioned closer to the splicing laser arc and the ARHCF is given a longitudinal offset of 125 µm from the center of the arc. Laser arc power of 5.5 W is used for 1.2 ms to splice the two fibers. The splice is performed in the absence of external pressurization of capillaries and yet, the fine structure in the cladding and the aspect ratio are completely preserved after splicing. The splice was strong enough to last through the rigor of the experiment, though it can be strengthened further if the O.D. of

ARHCF (160 µm) is matched with that of LMA-SCF (250 µm). Fig. 3a shows the longitudinal view of the splice under optical microscope and Fig. 3b shows the transverse cross-section of a broken splice point under SEM, confirming well-preserved ARHCF structure. The fiber end-faces were cleaved using *Fujikura CT-106* cleaver that can provide repeatable cleave angles of <0.5 ° for both fibers. The cleave parameters (clamp force, fiber tension) were customized by us for ARHCF end-face preparation.

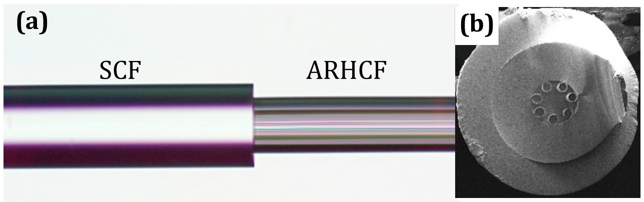

Fig. 3 a) Longitudinal view of the splice under an optical microscope, and b) transverse view of a broken splice point under SEM.

To test the coupling efficiency through the LMA-SCF and ARHCF splice, single moded laser output at 1.064 µm was launched into the fundamental mode of LMA-SCF using suitable mode-field adaptor, and power transmitted by 2 m long spliced ARHCF was measured. Fig. 4a shows the power exiting the ARHCF as a function of the power exiting the SCF at the splice point. The transmission efficiency (ratio of power exiting the ARHCF to power exiting SCF) was measured to be 89.1% corresponding to a coupling efficiency of 91.2%, considering the transmission loss (0.07 dB/m) of the fiber as per Fig. 1b. The beam quality of the light exiting ARHCF was characterized by $M^2 < 1.05$, confirming the transmitted light to be in the fundamental mode of ARHCF. The cleave angles for this splice were 0.1 ° for SCF and 0.2 ° for ARHCF, resulting in a compound cleave angle mismatch of 0.3 °. Considering the effect of cleave angle and mode field mismatch and no other misalignment, the expected maximum theoretical coupling efficiency between the power exiting SCF and that entering ARHCF is ~ 94%, which in good match with the observed value.

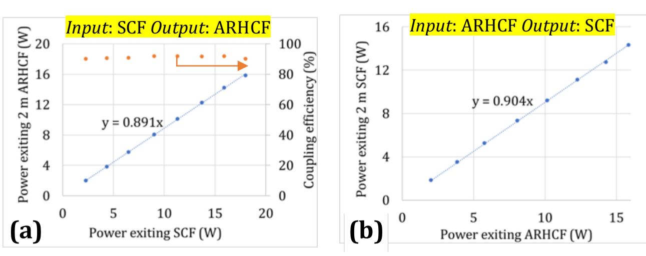

Fig. 4 *a*) Power transmitted by 2 m long ARHCF and coupling efficiency in the fundamental mode versus power exiting SCF *b*) Power transmitted by SCF versus power exiting ARHCF.

The propagation loss of the spliced ARHCF was measured by cutting back 1 m fiber length, and the measured value matched with the independent measurement of propagation loss of fundamental mode in long length of ARHCF (Fig. 1b). This confirms that only the fundamental mode propagated in the spliced ARHCF. The HOMs in the fabricated ARHCF are expected to propagate with at least >0.3 dB/m loss in our numerical simulations performed using full vector finite element modeling in COMSOL Multiphysics. Any core HOMs excited at splice point would lose their power thermally as they propagate along the fiber. The temperature at and near the splice point remained <30 °C for launched power of up to 18 W, confirming low power lost, and hence an efficient fundamental mode coupling. The power output was unaffected by bending of ARHCF up to bending diameters of 20 cm.

To improve the coupling efficiency further, we tested tapering the input end of ARHCF to reduce its MFD to match better with the LMA-SCF and have observed an improvement in coupling efficiency by 2%, which is in-line with the theoretical prediction. To test the reciprocity of splice, another piece of LMA-SCF (2 m long) was spliced at the output end of ARHCF and power transmitted through it was measured. The transmission efficiency through LMA-SCF was measured to be 90.4%, as shown in Fig. 4b. Since the SCF in this length scale has negligible transmission loss, the coupling efficiency can be assumed to be same as transmission efficiency in this case. The excellent reciprocity of splice loss is aligned with the theory and provides an easy technique for selectively exciting fundamental mode in an LMA-SCF that otherwise supports 12 guided core modes.

B. Integrating ARHCF with fiber laser cavity

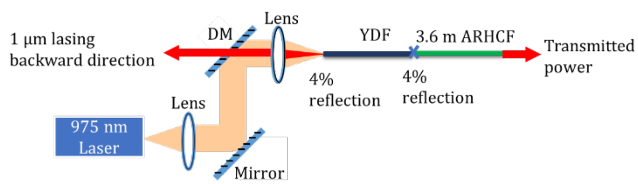

Fig. 5 Integrating spliced ARHCF in YDF laser cavity. DM: dielectric mirror reflecting 975 nm and transmitting wavelengths >1000 nm

The successful low loss splicing method was transferred to a fiber laser cavity. The ARHCF was spliced with a commercial YDF (Nufern YDF-25/250-VIII) having same fiber dimensions as the LMA-SCF considered in previous section. A 4%-4% linear laser cavity was built as per the experimental setup shown in Fig. 5. The cleave angles for both fibers at splice point were 0.2 °. Fresnel reflection at the glass-air interface at the input end of YDF and at the splice point with ARHCF formed the laser cavity. The laser cavity was cladding-pumped with a diode laser at 975 nm. Any residual pump power at the splice point would not propagate through ARHCF because of strong mode mismatch between the pump light and ARHCF core modes. Moreover, 975 nm lies in the resonant band of ARHCF and would suffer high propagation loss in the fiber. Therefore, the power transmitted out of ARHCF is purely the laser

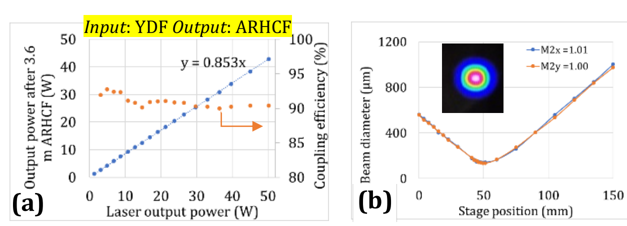

Fig. 6 *a*) Power transmitted through 3.6 m long ARHCF and coupling efficiency versus laser output power; b) M^2 measurement of transmitted beam *Inset:* Mode profile of output beam

output, which was also confirmed by measurement of output spectrum using optical spectrum analyzer.

The YDF was coiled with 8.5 cm bend diameter and both of its end-faces were flat cleaved with cleave angle of 0.2 °, leading to a symmetric cavity. The laser output from YDF, in the absence of spliced ARHCF, was characterized by slope efficiency of 47.6% and M^2_{mean} = 1.07 in both forward and backward directions with less than 1% difference in power levels. Therefore, in these experiments, we have simultaneously measured the power and beam quality for beam exiting ARHCF and for laser output in backward direction (pump input end of YDF). Fig. 6a shows the power transmitted through 3.6 m long ARHCF versus a variation in laser output power. The transmission efficiency is found to be 85.3%, corresponding to a coupling efficiency of 90.4% into the fundamental mode for CW power of 50.2 W. Consistent coupling efficiency was observed across the available laser power as presented in Fig. 6a. Fig. 6b show the beam quality measurement of the transmitted beam through ARHCF, which is characterized by M^2_{xy} = 1.01 and 1.00, respectively. The slight improvement in M^2 after propagation through ARHCF is the result of filtering of any HOMs that were present in the coupled laser beam.

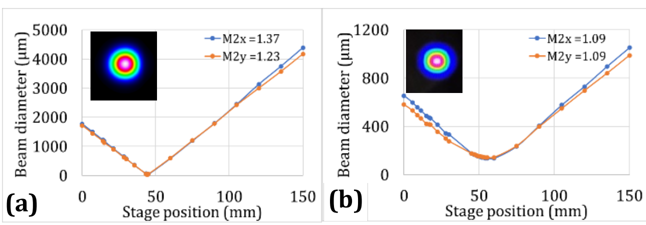

Fig. 7 M^2 measurement of *a*) direct laser output beam *b*) beam exiting ARHCF

To investigate this effect further and show its potential application in spatial filtering of laser beam to improve beam quality, we adjusted the YDF bending so that the laser output is characterized by a higher M^2_{mean} = 1.30 (Fig. 7a) without the ARHCF. In this configuration, the transmission efficiency through ARHCF drops down to 81.5% for coupled power of 52.2 W because of the higher loss suffered by HOMs in ARHCF. The power exiting the ARHCF is characterized by M^2_{mean} = 1.09 (Fig. 7b), which clearly implies that propagation through ARHCF can improve the beam quality at the cost of some power loss. We should mention that the ARHCF used was not specifically fabricated for HOM suppression, and its higher order mode extinction ratio (HOMER) is only ~6 for the first HOM. Hence, the HOMs are not completely suppressed within the given length. By designing the capillary diameter ~0.68 times the core diameter, HOMER that is greater than 1000 can be obtained in an ARHCF without affecting the propagation loss in the fundamental mode [10]. We believe such fibers are suitable candidates for high power laser beam delivery. We plan to investigate further in this direction by fabricating an ARHCF with high HOMER and explore its potential for improving the laser beam quality as a spatial mode filter [21].

4. CONCLUSIONS

We reported the first demonstration of >90% coupling efficiency into fundamental mode of a single ring ARHCF using fusion splicing with a solid core fiber. We discussed the effects of mode matching and cleave angle on coupling efficiency. The same design principles can be extended to any larger mode area ARHCFs, as well as nested antiresonant fibers. The spliced ARHCF is also integrated in a YDF laser cavity for beam delivery through fusion splicing. We achieved low loss, efficient laser beam delivery with coupling efficiency of 90.4% for launched powers of over 50 W. Although our experiments were constrained to CW laser, we believe that the operating principle holds for delivery of ultrashort pulses as well. Direct splicing of active fiber with ARHCF opens potential avenues for utilizing the modal characteristics of ARHCF for enhancing the performance of high-power CW and ultrafast pulsed fiber lasers.

Funding. National Research Foundation Singapore, Quantum Engineering Programme.

Disclosures. The authors declare no conflicts of interest.

References

1. J. Knight, D. Hand and F. Yu, "Hollow-Core Optical Fibers Offer Advantages at Any Wavelength", Photonics Spectra, April 2019
2. Xinyue Zhu, Dakun Wu, Yazhou Wang, Fei Yu, Qiurui Li, Yunfeng Qi, Jonathan Knight, Shufen Chen, and Lili Hu, Opt. Express **29**, 1492-1501 (2021)
3. C. Goel, J. Zang, M. Parrot and S. Yoo, J. Lightwave Technol. **39** (12), 3998-4005 (2021),
4. H. Sakr, Y. Hong, T. D. Bradley, G. T. Jasion, J. R. Hayes, H. Kim, I. A. Davidson, E. Numkam Fokoua, Y. Chen, K. R. H. Bottrill, N. Taengnoi, N. V. Wheeler, P. Petropoulos, D. J. Richardson, and F. Poletti, J. Lightwave Technol. **38**, 159-165 (2020)
5. M. Gebhardt, C. Gaida, T. Heuermann, F. Stutzki, C. Jauregui, J. Antonio-Lopez, A. Schulzgen, R. Amezcua-Correa, J. Limpert, and A. Tünnermann, Opt. Lett. **42**, 4179-4182 (2017)
6. B. Debord, F. Amrani, L. Vincetti, F. Gérôme and F. Benabid, Fibers **7**(2), 16 (2019)
7. M. A. Duguay, Y. Kokubun, T. L. Koch and L. Pfeiffer L., Appl. Phys. Lett. **49**(1), 13 (1986)
8. L. Vincetti and V. Setti, Opt. Express **18**, 23133–23146 (2010).
9. W. Belardi and J. C. Knight, Opt. Express **21**, 21912-21917 (2013)
10. P. Uebel, M. C. Günendi, M. H. Frosz, G. Ahmed, N. N. Edavalath, J. -M. Ménard, and P. St. J. Russell, Opt. Lett. **41**, 1961-1964 (2016)
11. M. Michieletto, J. K. Lyngsø, C. Jakobsen, J. Lægsgaard, O. Bang, and T. T. Alkeskjold, Opt. Express **24**, 7103-7119 (2016)
12. X. Zheng, B. Debord, L. Vincetti, B. Beaudou, F. Gérôme, and F. Benabid, Opt. Express **24**, 14642-14647 (2016)
13. I. A. Bufetov, A. N. Kolyadin, A. F. Kosolapov, V. P. Efremov, and V. E. Fortov, Opt. Express **27**, 18296-18310 (2019)
14. Y. Min, A. Filipkowski, G. Stępniewski, D. Dobrakowski, J. Zhou, B. Lou, M. Klimczak, L. Zhao, and R. Buczyński, J. Lightwave Technol. **39**(10), 3251-3259 (2021)
15. W. Huang, Y. Cui, X. Li, Z. Zhou, Z. Li, M. Wang, X. Xi, Z. Chen, and Z. Wang, Opt. Express **27**, 37111-37121 (2019)
16. W. Huang, X. Ye, Y. Cui, Z. Zhou, Z. Chen, Z. Wang, J. Chen, Proc. SPIE 11849, Fourth International Symposium on High Power Laser Science and Engineering (HPLSE 2021), 118490I (6 June 2021)
17. A. Ghatak, and K. Thyagarajan, (1998). An Introduction to Fiber Optics. Cambridge: Cambridge University Press.
18. C. M. Harvey, F. Yu, J. C. Knight, W. J. Wadsworth and P. J. Almeida, IEEE Photon. Technol. Lett. **28**(6) 669-672, (2016),
19. H. Lim, A. Chong, and F. W. Wise, Opt. Express **13**, 3460-3464 (2005)
20. N. Simakov, A. V. Hemming, A. Carter, K. Farley, A. Davidson, N. Carmody, M. Hughes, J. M. O. Daniel, L. Corena, D. Stepanov, and J. Haub, Opt. Express **23**, 3126-3133 (2015)

21. P. Patimisco, A. Sampaolo, L. Mihai, M. Giglio, J. Kriesel, D. Sporea, G. Scamarcio, F. K. Tittel, and V. Spagnolo, Sensors (Basel) **16**(4), 533 (2016)

Reference List with Titles

1. J. Knight, D. Hand and F. Yu, "Hollow-Core Optical Fibers Offer Advantages at Any Wavelength", Photonics Spectra, April 2019
2. Xinyue Zhu, Dakun Wu, Yazhou Wang, Fei Yu, Qiurui Li, Yunfeng Qi, Jonathan Knight, Shufen Chen, and Lili Hu, "Delivery of CW laser power up to 300 watts at 1080 nm by an uncooled low-loss anti-resonant hollow-core fiber," Opt. Express 29, 1492-1501 (2021)
3. C. Goel, J. Zang, M. Parrot and S. Yoo, "Temperature-Insensitive Mechanical Sensor Using Multi-Modal Behavior of Antiresonant Hollow-Core Fibers," J. Lightwave Technol. 39 (12), 3998-4005 (2021),
4. H. Sakr, Y. Hong, T. D. Bradley, G. T. Jasion, J. R. Hayes, H. Kim, I. A. Davidson, E. Numkam Fokoua, Y. Chen, K. R. H. Bottrill, N. Taengnoi, N. V. Wheeler, P. Petropoulos, D. J. Richardson, and F. Poletti, "Interband Short Reach Data Transmission in Ultrawide Bandwidth Hollow Core Fiber," J. Lightwave Technol. 38, 159-165 (2020)
5. M. Gebhardt, C. Gaida, T. Heuermann, F. Stutzki, C. Jauregui, J. Antonio-Lopez, A. Schulzgen, R. Amezcua-Correa, J. Limpert, and A. Tünnermann, "Nonlinear pulse compression to 43 W GW-class few-cycle pulses at 2 µm wavelength," Opt. Lett. 42, 4179-4182 (2017)
6. B. Debord, F. Amrani, L. Vincetti, F. Gérôme and F. Benabid, "Hollow-Core Fiber Technology: The Rising of "Gas Photonics", Fibers 7(2), 16 (2019)
7. M. A. Duguay, Y. Kokubun, T. L. Koch and L. Pfeiffer L., "Antiresonant reflecting optical waveguides in SiO2-Si multilayer structures," Appl. Phys. Lett. 49(1), 13 (1986)
8. L. Vincetti and V. Setti, "Waveguiding mechanism in tube lattice fibers," Opt. Express 18, 23133–23146 (2010).
9. Walter Belardi and Jonathan C. Knight, "Effect of core boundary curvature on the confinement losses of hollow antiresonant fibers," Opt. Express 21, 21912-21917 (2013)
10. P. Uebel, M. C. Günendi, M. H. Frosz, G. Ahmed, N. N. Edavalath, J. -M. Ménard, and P. St. J. Russell, "Broadband robustly single-mode hollow-core PCF by resonant filtering of higher-order modes," Opt. Lett. 41, 1961-1964 (2016)
11. M. Michieletto, J. K. Lyngsø, C. Jakobsen, J. Lægsgaard, O. Bang, and T. T. Alkeskjold, "Hollow-core fibers for high power pulse delivery," Opt. Express 24, 7103-7119 (2016)
12. X. Zheng, B. Debord, L. Vincetti, B. Beaudou, F. Gérôme, and F. Benabid, "Fusion splice between tapered inhibited coupling hypocycloid-core Kagome fiber and SMF," Opt. Express 24, 14642-14647 (2016)
13. I. A. Bufetov, A. N. Kolyadin, A. F. Kosolapov, V. P. Efremov, and V. E. Fortov, "Catastrophic damage in hollow core optical fibers under high power laser radiation," Opt. Express 27, 18296-18310 (2019)
14. Y. Min, A. Filipkowski, G. Stępniewski, D. Dobrakowski, J. Zhou, B. Lou, M. Klimczak, L. Zhao, and R. Buczyński, "Fusion Splicing of Silica Hollow Core Anti-Resonant Fibers with Polarization Maintaining Fibers," J. Lightwave Technol. 39(10), 3251-3259 (2021)
15. W. Huang, Y. Cui, X. Li, Z. Zhou, Z. Li, M. Wang, X. Xi, Z. Chen, and Z. Wang, "Low-loss coupling from single-mode solid-core fibers to anti-resonant hollow-core fibers by fiber tapering technique," Opt. Express 27, 37111-37121 (2019)
16. W. Huang, X. Ye, Y. Cui, Z. Zhou, Z. Chen, Z. Wang, J. Chen, "High power laser coupling from solid-core fibers to anti-resonant hollow-core fibers by fiber tapering technology," Proc. SPIE 11849, Fourth International Symposium on High Power Laser Science and Engineering (HPLSE 2021), 118490I (6 June 2021)
17. A. Ghatak, and K. Thyagarajan, (1998). An Introduction to Fiber Optics. Cambridge: Cambridge University Press.
18. C. M. Harvey, F. Yu, J. C. Knight, W. J. Wadsworth and P. J. Almeida, "Reduced Repetition Rate Yb3+ Mode-Locked Picosecond Fiber Laser With Hollow Core Fiber," IEEE Photon. Technol. Lett. 28(6) 669-672, (2016),
19. Hyungsik Lim, Andy Chong, and Frank W. Wise, "Environmentally-stable femtosecond ytterbium fiber laser with birefringent photonic bandgap fiber," Opt. Express 13, 3460-3464 (2005)
20. N. Simakov, A. V. Hemming, A. Carter, K. Farley, A. Davidson, N. Carmody, M. Hughes, J. M. O. Daniel, L. Corena, D. Stepanov, and J. Haub, "Design and experimental demonstration of a large pedestal thulium-doped fibre," Opt. Express 23, 3126-3133 (2015)
21. P. Patimisco, A. Sampaolo, L. Mihai, M. Giglio, J. Kriesel, D. Sporea, G. Scamarcio, F. K. Tittel, and V. Spagnolo, "Low-Loss Coupling of Quantum Cascade Lasers into Hollow-Core Waveguides with Single-Mode Output in the 3.7-7.6 µm Spectral Range," Sensors (Basel) 16(4), 533 (2016)